Available online at www.sciencedirect.com

ScienceDirect

Procedia CIRP 58 (2017) 152 – 157

www.elsevier.com/locate/procedia

16th CIRP Conference on Modelling of Machining Operations

Modelling of cutting process impact on machine tool thermal behaviour based on experimental data

Martin Mareš[a,]*, Otakar Horejš[a]

[a]*Czech Technical University in Prague, Faculty of Mechanical Engineering, Department of Production Machines and Equipment, RCMT, Horská 3, 128 00 Prague, Czech Republic*

* Corresponding author. Tel.: +420-221-990-936; fax: +420-221-990-999. *E-mail address:* m.mares@rcmt.cvut.cz

Abstract

Achieving high workpiece accuracy is a long-term goal of machine tool designers. There are many causes of workpiece inaccuracy, with thermal errors being the most dominant. An indirect compensation (using predictive models) is a promising strategy to reduce thermal errors without increasing machine tool cost. The most significant drawback is that the majority of applied models presume machines operate under load-free conditions without any reference to cutting processes. This article aims to extend the model validity by accounting for cutting process influence and verify the model during experiments involving different tools and cutting parameters. Moreover, several compensation model structures are considered.

Peer-review under responsibility of the scientific committee of The 16th CIRP Conference on Modelling of Machining Operations

Keywords: Machine tool; Cutting process; Thermal error; Real-time compensation

1. Introduction

Thermally induced displacements at the tool center point (TCP) of a machine tool (MT) structure cannot be sufficiently reduced by design concept and/or by temperature control without high additional costs. On the contrary, indirect (software) compensation of thermally induced displacements at the TCP is one of the most widely employed techniques to reduce MT thermal errors due to its cost-effectiveness and ease of implementation.

Ordinarily, approximation models are based on measured auxiliary variables [1] (temperatures, spindle speed, etc.) used for calculation of the resulting thermally induced displacements at the TCP. Many strategies were investigated to establish the models, e.g. multiple linear regressions [2], artificial neural networks [3], transfer functions (TF) [4, 5], etc. (for more details see [6, 7]).

Although real-time software compensations of thermal errors exist, these compensations have a number of serious drawbacks. The majority of these models only presume MTs under load-free rotation of the main spindle (air cutting) without any reference to the cutting process despite its essential impact on workpiece accuracy [1].

Thermal distortion under the spindle load condition was investigated using a stressing unit in [8]. A robust compensation of MT thermal errors in consideration of rough machining was developed but verification on real cutting processes is missing. The result of [9] showed that the prediction accuracy of solely air cutting models are unacceptable in real cutting applications. Methods to compensate for MT thermal errors should include cutting process effects to ensure their robustness.

In [5] a general approach was introduced to dynamic thermal errors modelling (based on TF) of MT under load-free conditions. This approach was successfully applied to 3 different MT structures. The work was extended to the real cutting process description based on measured spindle power carried out on a 3-axis vertical milling centre under rough machining [10]. In this article the approach is applied to a 5-axis milling machine and the effectiveness of three compensation model structures during various cutting processes are tested.

Peer-review under responsibility of the scientific committee of The 16th CIRP Conference on Modelling of Machining Operations
doi:10.1016/j.procir.2017.03.208

2. Experimental setup

MT thermal deformations measured between the workpiece surface and TCP (δ_{TCP}) generally consist of three elements (according to eq.(1)): MT **frame** deformation (δ_{frame}; influence of feed drive activity, spindle bearings, removed material, ambient temperature etc.), **tool** elongation (δ_{tool}; impact of cutting process) and **workpiece** deformation ($\delta_{workpiece}$).

$$\delta_{TCP} = \delta_{frame} + \delta_{tool} + \delta_{workpiece} \quad (1)$$

A model of the MT frame thermal deformation is provided by previous work [5] and analysis of workpiece deformation is out of scope of this article. This paper mainly focuses on issues concerning tool thermal elongation.

All experiments were performed on a 5-axis milling centre with a 630 mm rotary table diameter. The MT was equipped with a number of temperature probes (Pt100, Class A, 3850 ppm/K) placed close to thermal sinks and sources. These probes were primarily used for safety purposes and were installed directly into the MT control system. Two from the discussed probes along with a spindle power record $P_{spindle}$ were utilised in the thermal deformation modelling process. These probes were namely $T_{spindle}$ (temperature of spindle bearings) and $T_{ambient}$ (temperature of the MT surrounding). Additionally, the MT was equipped with an industrial infrared (IR) temperature sensor (Optris CT-SF15-C1) T_{tool} for non-contact monitoring of tool temperature development during the cutting process and following phases. The body of the sensor and its cabling was safely covered in a flexi hose, which is commonly used for cooling liquid circuits.

Positions of thermal probes, a workpiece (solid cylindrical shape) placement and measuring positions of the spindle and a tool in the MT workspace are depicted in Fig.1(a).

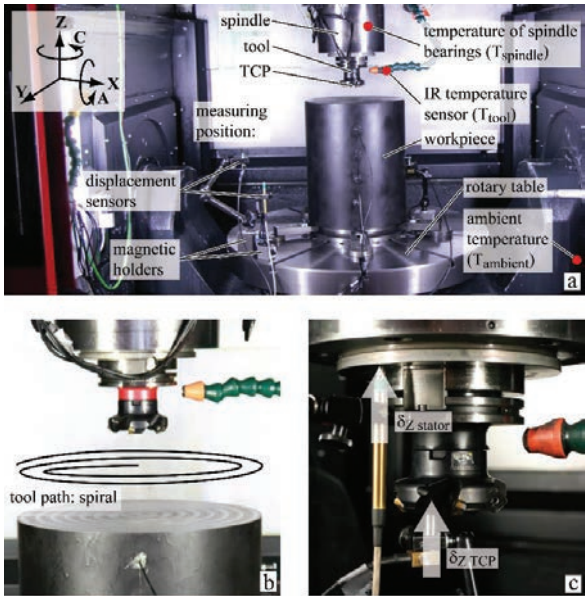

Fig. 1. Experimental setup on 5-axis milling machine; overview (a), cutting process (b), measuring position (c).

The MT should be in a steady state with its surrounding as a precondition to initiate the testing. All experiments include a load phase (cutting process) followed by a cool-down phase. The load phase of the testing consists of cycle repetition of two parts: cutting (Fig.1(b)) and measuring (Fig.1(c)). The **cutting part** means removal of one layer of workpiece material by following a specific tool path. The tool path was set up as a spiral for an even spindle load during cutting. The **measuring part** (deformations were recorded only in the most affected *Z* direction) following the cutting was executed with the help of two inductive contact sensors recording displacement of the MT frame (measured at the stator part of the spindle, further denoted as $\delta_{Z\ stator}$) and TCP ($\delta_{Z\ TCP}$). The sensors were mounted in magnetic holders attached to the MT table. The cutting and measuring parts were repeated in the load phase until supposed achievement of MT steady state with all active thermal sinks and sources (up to 6 hours). The cooling phase followed with the permanent spindle placement in the measuring position (Fig.1(c)). The MT was in a feed-drive-on mode during the cool-down phase.

The demanded value of the tool thermal elongation ($\delta_{Z\ tool}$) was obtained by the difference between the two measured deformational elements:

$$\delta_{Ztool} = \delta_{ZTCP} - \delta_{Z\,stator} \quad (2)$$

Three different tools were used for individual tests:

- Ø25 mm - finishing process,
- Ø63 mm - semi-finishing process and
- Ø100 mm - rough machining.

All results and conclusions are closely associated with conditions of experiments:

- cutting process is only face milling,
- dry machining,
- workpiece material is medium-carbon steel 1.0503.

3. Compensation models of thermal errors

A discrete TF was used to describe the link between the excitation (temperature, spindle power) and its response (thermal displacement). The differential form of the TF in the time domain is introduced in eq.(3):

$$y(k) = \frac{u(k-n)\cdot a_n + \cdots + u(k-1)\cdot a_1}{b_0} + \\ + \frac{u(k)\cdot a_0 - y(k-m)\cdot b_m - \cdots - y(k-1)\cdot b_1}{b_0}, \quad (3)$$

where *u(k)* is a TF input vector in time domain, *y(k)* is an output vector in time domain, a_n are parameters-to-be-identified of the TF input and b_m of the TF output, *k-n* (*k-m*) means the n-multiple (m-multiple) delay in sampling frequency. Linear parametric models of ARX (autoregressive with external input) or OE (output error) were used for the parameter estimations. The stability of each TF was examined

through a step response. The approximation quality of the simulated behaviour is shown in eq.(4). This value expresses the percentage of the output variation that is reproduced by the model [11].

$$fit = \left(1 - \frac{\left\|Y - \hat{Y}\right\|}{\left\|Y - \bar{Y}\right\|}\right) \cdot 100 \tag{4}$$

The error of approximation is shown in eq. (5).

$$residue = Y - \hat{Y} \tag{5}$$

The Y value in eq.(4) and eq.(5) represents a measured output (thermal deformation), $\hat{Y}$ is a simulated (predicted) model output and $\bar{Y}$ in eq.(3) expresses arithmetic mean over the time of the measured output.

The next table summarizes the cutting parameters of a calibration test: tool diameter (D), total number of teeth in cutter (z_n), working engagement (a_e), depth of cut (a_p), table feed (v_f), spindle speed (n), average spindle power ($\bar{P}_{spindle}$) and chosen tool path (see Fig.1(b)).

Table 1. Cutting parameters during calibration test.

D	z_n	a_e	a_p	v_f	n	$\bar{P}_{spindle}$
[mm]		[mm]	[mm]	[m/min]	[rpm]	[kW]
63	5	31.5	1.5	758	758	0.3

3.1. Load-free model

A load-free model of MT thermal errors is supposed to cover thermal displacements of the MT frame ($\delta_{Z\,stator}$).

A load-free model introduced in a previous work [5] is used here with the aforementioned intention. The model was calibrated in [5] to approximate deformational impacts of main thermal sinks and sources affecting the MT frame: spindle bearings and ambient temperature. The model structure operating in Z direction of the MT is expressed in eq.(6). The load-free model would be an integral part of the models that include cutting process.

$$\delta_{Z\,stator}(\text{model}) = \Delta T_{spindle} \cdot \varepsilon_1 + \Delta T_{ambient} \cdot \varepsilon_2, \tag{6}$$

where $\delta_{Zstator}$ (model) is the approximation value of the thermal deformation measured at the stator part of the spindle in Z direction, $\Delta T_{spindle}$ and $\Delta T_{ambient}$ are temperature inputs in relative coordinates, ε_1 is TF approximating influence of spindle rotation and ε_2 is TF approximating influence of MT surrounding. Parameters of identified TF [5] are summarized in Table 2.

The load-free model (eq.(6)) was verified within the calibration test (see Table 1). Measured behaviours of inputs into the compensation model (along with spindle power and tool temperature) are shown in Fig. 2(a). The drop in measured behaviour of the tool temperature followed a necessary tool change after wearing of tool inserts.

The result of the load-free model application on measured data regarding the spindle stator part is depicted in Fig.2(b). Residual deformations along with *fit* value 76% confirm the load-free model applicability.

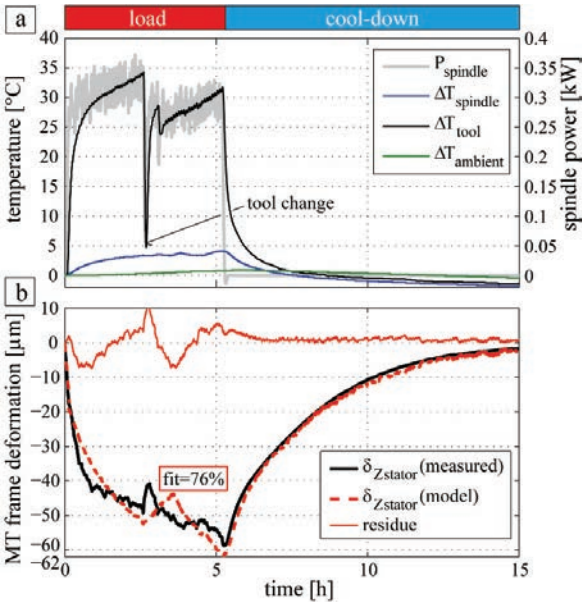

Fig. 2. Calibration test: stator part, 0.3 kW, Ø63 mm; inputs (a), outputs (b).

3.2. Models including cutting process

Three model structures were built up to approximate MT thermal errors at TCP including the cutting process. The basic idea of the model's structure is a linearization of the MT thermal behaviour by superposition of participating deformational elements on resultant TCP deflection as expressed by eq.(1). The base of all three structures is explained by load-free model (eq.(6)).

The first *model A* approximates thermal deformation at TCP by simply multiplying the load-free model. *Model A* requires neither additional calibration nor other external measuring gauges. The model is expressed by eq.(7). Its application on calibration measurement (Figure 2(a)) is shown in Figure 3.

$$\delta_{Z\,TCP}(\text{model A}) = K \cdot \delta_{Z\,stator}(\text{model}) \tag{7}$$

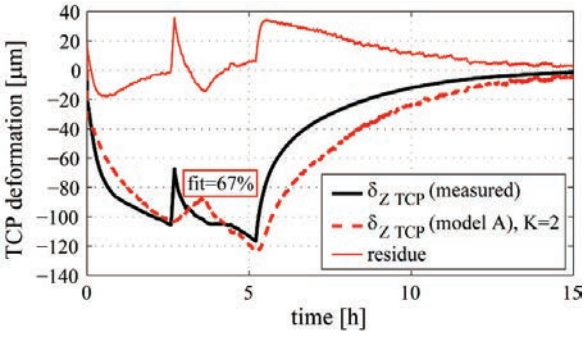

Fig. 3. Calibration test: TCP, 0.3 kW, Ø63 mm; model A application.

The thermal error *model B* uses actual spindle power value taken directly from the MT control system; P_{spindle} is the model input used to determine the tool thermal elongation. The input does not have clear linear dependence with the thermal deformation and this model type requires additional calibration measurements (for each used tool at least) though without any extra measuring gauge. The model is formulated in eq.(8).

$$\delta_{Z\,TCP}(\text{model B}) = \delta_{Z\,stator}(\text{model}) + (P_{spindle} \cdot \gamma_1) \cdot k_i, \quad where\ i = 1,2. \tag{8}$$

The last thermal error model (*model C*) operates with temperature measured on a tool's surface. ΔT_{tool} is the input into the model's part dealing with the tool thermal elongation. *Model C* requires one additional calibration measurement and the extra measuring device (IR temperature sensor; see Fig.1(a)). However, the linear dependence between the model input and output is observable through all examined cutting processes. The mathematical expression of the model is as follows:

$$\delta_{Z\,TCP}(\text{model C}) = \delta_{Z\,stator}(\text{model}) + \Delta T_{tool} \cdot \varepsilon_3 \tag{9}$$

The $\delta_{Z\,TCP}$ (*model A*), $\delta_{Z\,TCP}$ (*model B*) and $\delta_{Z\,TCP}$ (*model C*) in eq.(7) to eq.(9) are approximation values of the thermal deformations measured at TCP in *Z* direction. Multiplying constant *K* in eq.(7) was obtained experimentally and is equal to 2 (see Fig.3). The TF γ_1 in eq.(8) approximates the tool thermal elongation with spindle power as the input value. Experimentally obtained coefficient $k_1 = 1$ is applied for 25 mm and 63 mm diameter tools and $k_2 = 0.4$ for 100 mm diameter tool in eq.(8). The TF ε_3 in eq.(9) approximates the tool thermal elongation with tool temperature as the input value.

Outputs of identified TF γ_1 and ε_3 from eq.(8) and eq.(9) covering a tool's thermal elongation (given by eq.(2) from measured data) during the calibration measurement are presented in Fig.4. Behaviours of the model input values remain the same as shown in Fig. 2(a). Parameters of the identified TF are summarised in Table 2.

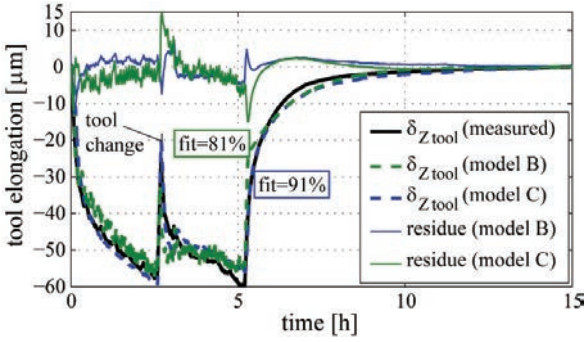

Fig. 4. Calibration test: tool elongation, 0.3 kW, Ø63 mm; model B and model C calibration.

Following table summarizes the parameters of identified TF used in eq.(6) to eq.(9).

Table 2. Parameters of identified transfer functions.

TF	a_0	a_1	a_2	b_0	b_1	b_2
ε_1	-2.6573	5.1965	-2.5392	1	-1.9865	0.9865
ε_2	-8.428	8.4279	0	1	-0,6913	-0,3087
ε_3	-0.4099	0.1057	0.2872	1	-0.2835	-0.7063
γ_1	-1.3928	1.3923	0	1	-1.9855	0.9855

4. Verification of modelling approaches

The setups of model verification experiments involving the cutting process were mainly chosen from comparison of different processes (finishing, semi-finishing and rough machining) point of view. The model's ability to linearize MT thermal issue was examined.

4.1. Finishing

A tool diameter of 25 mm was selected for performance on a finishing test. The set of cutting parameters of the test can be seen in Table 3. The verification test was selected as representative for finishing process with a low value of the average spindle power. The experiment also verified the load-free model's validity within the finishing processes.

4.2. Semi-finishing

Models of MT thermal errors (eq.(6) to eq.(9)) were further applied to a test in terms of similar cutting process (semi-finishing) to the calibration measurement. The verification experiment differs from the calibration only by the depth of cut value (a_p, see Table 1 and Table 3) causing higher average spindle power (0.4 kW).

4.3. Rough machining

Two rough machining verification tests were carried out with the help of a 100 mm diameter tool. The set of cutting parameters of the last two tests are also presented in Table 3.

The first test was designed as an additional calibration test for identification of coefficient k_2 in eq.(8). The last verification test was selected as a representative for rough machining with higher value of the spindle power (2.5 kW).

Table 3. Cutting parameters during verification tests.

D [mm]	z_n	a_e [mm]	a_p [mm]	v_f [m/min]	n [rpm]	$\bar{P}_{\text{spindle}}$ [kW]
25	3	18.75	0.1	764	2546	0.006
63	5	31.5	2.5	758	758	0.4
100	7	50	0.6	668	477	0.7
100	7	50	3	668	477	2.5

Measured behaviours of inputs into the compensation models during the finishing process are shown in Fig. 5(a), during the semi-finishing process in Fig. 5(b) and during the rough machining processes in Fig. 5(c) and Fig. 5(d). The last test is consisted of a load phase only. A cool-down phase has not been recorded due to a lack of time.

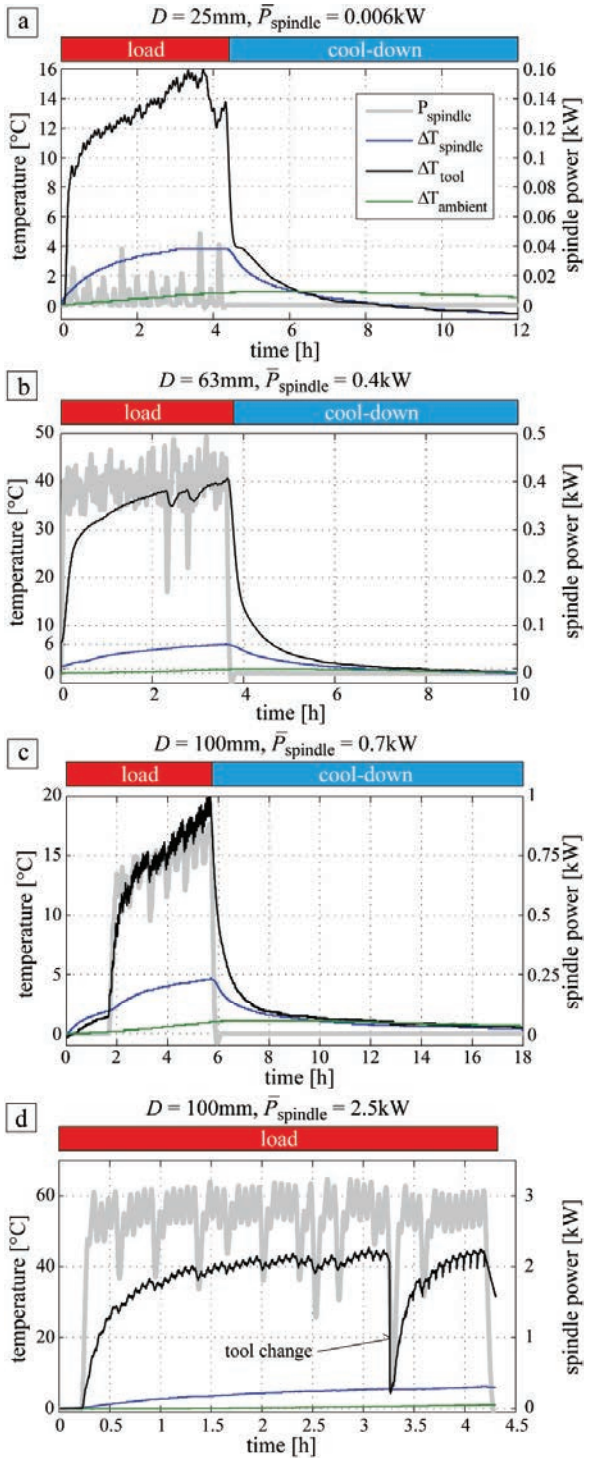

Fig. 5. Measured model inputs during verification tests; finishing (a), semi-finishing (b), rough machining (c) and (d).

Measured deformations at the TCP and the stator part of the spindle in *Z* direction during finishing process are depicted in Fig. 6(a), during the semi-finishing process in Fig. 6(b) and during the rough machining processes in Fig. 6(c) and Fig. 6(d). The Figures also contain behaviours of residual deformations (eq.(5)) obtained by model applications of measured data. The residues represent an MT deformational state after compensation by introduced approaches from eq.(7) to eq.(9).

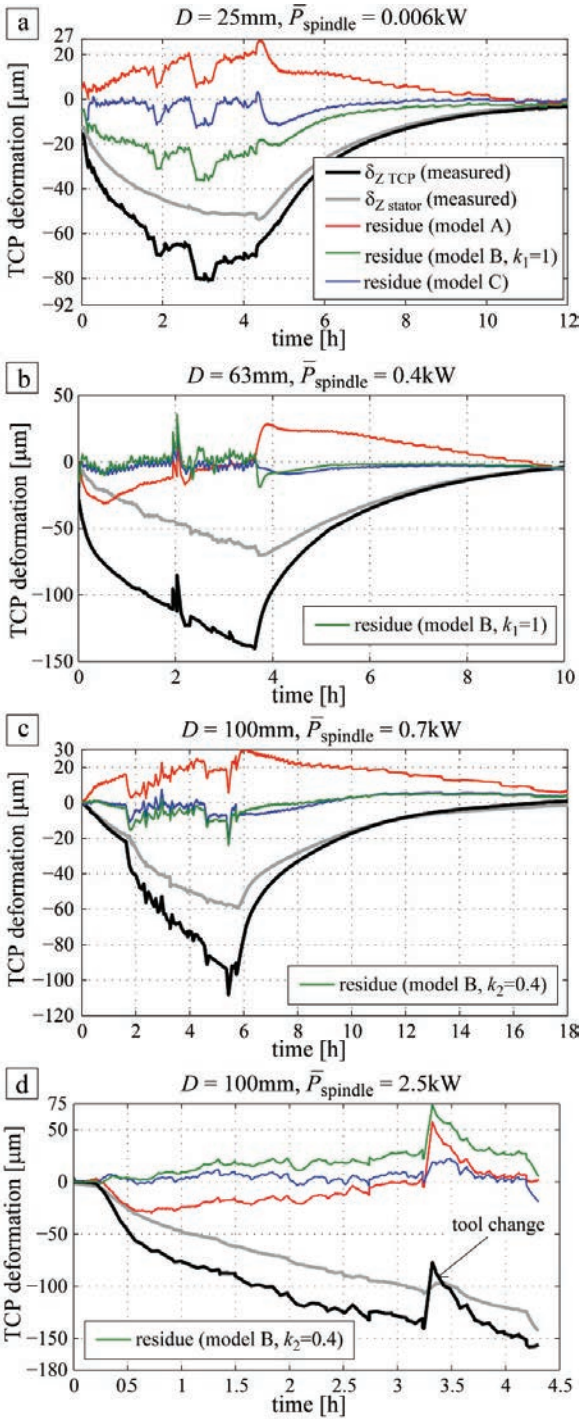

Fig. 6. Results of verification tests; finishing (a), semi-finishing (b), rough machining (c) and (d).

5. Conclusions

A load-free compensation model of MT thermal errors [5] was extended to include a cutting process. The experiments involving cutting processes were performed on a 5-axis milling machine with a 630 mm table diameter. Experiments were carried out under specific conditions: cutting process was face milling, no process liquid was used and the material of the workpiece was medium-carbon steel 1.0503. Three models of MT thermal behaviour based on TF were designed. Models were applied to data recorded on TCP during tests of different cutting processes: finishing, semi-finishing and rough machining. Various cutting tools were selected for executing each cutting process. Benefits (and disadvantages) of the compensation models are further discussed.

Model A (eq.(7)) needs no additional calibration tests. Model is able to make predictions without any extra measuring gauges (only inputs taken from MT control system). Its outcome has an inferior approximation quality (see Table 4) but still significantly improves on the MT initial state (compare Fig.7(a) and (b)). The model structure consists of multiplied load-free model by constant K=2. From the results presented in Fig.6 it is possible to claim that the separate cutting process impact on TCP thermal errors in Z direction is around 50%.

Model B (eq.(8)) needs an additional time-consuming calibration test for each tool used. The discussed MT thermal issue has been approximated by linear combination of *model B* outcomes (solving tool thermal elongation part) and a set of gain coefficients k_i. Limits of the model applicability are exceeded in the case of the finishing cutting process where the model outcome is covering only the stator part of the spindle (see Fig.6(a)). This is due to a weak input signal (spindle power). The model showed an insignificant reaction to tool change, as shown in Fig.6(d). The model works without any extra measuring gauges. This model typically provides higher approximation quality compared to the previous model (see Table 4).

Model C (eq.(9)) requires only one additional calibration test of cutting process impact on tool thermal elongation. This modelling approach proves a good linear relation between temperatures measured on MT structure and MT thermal errors. It was necessary to employ one extra measuring device for non-contact sensing of tool temperature. Model outcomes were attained with highest approximation quality (see Table 4).

Peak-to-peak values (difference between maximum and minimum of whole recorded deformations or calculated residues during one experiment) were compared to *fit* values and are presented in Table 4.

Table 4. Summary of model's approximation quality.

D	$P_{spindle}$	fit [%]			peak-to-peak [µm]			
[mm]	[kW]	*A*	*B*	*C*	*initial*	*A*	*B*	*C*
25	0.006	65	49	86	81	27	36	15
63	0.3	67	90	92	116	61	21	10
63	0.4	76	87	86	140	52	29	14
100	0,7	48	84	85	97	32	20	18
100	2.5	54	72	81	158	86	74	41
average		62	76	86	118	51	36	20

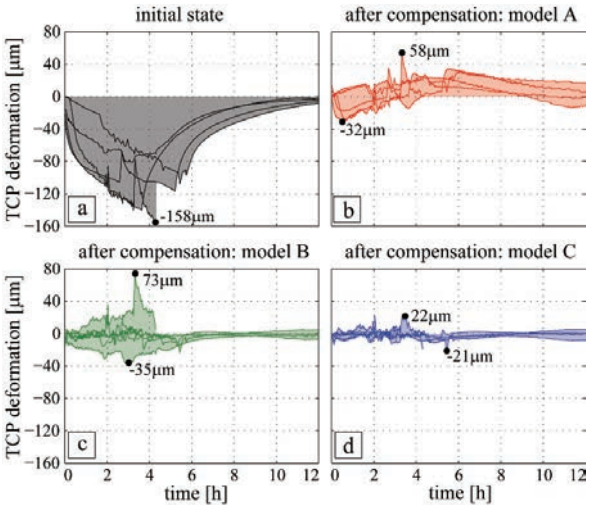

Fig. 7. Achieved results through all executed tests.

Further research should be conducted on the topic of cutting process impact on MT thermal errors (e.g. tests with different workpiece material, wet machining, different technology, etc.).

Acknowledgements

This paper (Modelling of cutting process impact on machine tool thermal behaviour based on experimental data) has received funding from the Technology Agency of the Czech Republic (Project TE01020075).

References

[1] Brecher C., Wissmann A. Compensation of thermo-dependent machine tool deformations due to spindle load: investigation of the optimal transfer function in consideration of rough machining. Prod. Eng. Res. Devel., 5, 2011. p. 565−574.

[2] Postlethwaite S., Allen J., Ford D. The use of thermal imaging, temperature and distortion models for machine tool thermal error reduction, Proc. Inst. Mech. Eng. Pt. B: J. Eng. Manuf., 212/8, 1998. p. 671−679.

[3] Mize C., Ziegert J. Neural network thermal error compensation of a machining center. Precision Engineering, 24/4, 2000. p. 338−346.

[4] Brecher C., Hirsch P. Compensation of thermo-elastic machine tool deformation based on control internal data. CIRP Annals - Manufacturing Technology, 53/1, 2004. p. 299−304.

[5] Horejš O., Mareš M., Hornych J. A general approach to thermal error modelling of machine tools. Machines et Usinage à Grande Vitesse (MUGV), Clermont Ferrand, France, 2014.

[6] Bryan J. International status of thermal error research. CIRP Annals - Manufacturing Technology, 39/2, 1990. p. 645−656.

[7] Mayr J., Jedrzejewski J., Uhlmann E., Donmez M.A., Knapp W., Härtig F., Wendt K., Moriwaki T., Shore P., Schmitt R., Brecher C., Würz T., Wegener K. Thermal issues in machine tools. CIRP Annals - Manufacturing Technology, 61/2, 2012. p. 771−791.

[8] Brecher C., Wissmann A. Stressing unit for modelling of thermal behaviour of a milling machine. 12th CIRP Conference on Modelling of Machining Operations, Donostia - San Sabastian – Spain, 2009.

[9] Chen J.S. A study of thermally induced machine tool errors in real cutting conditions. Int. J. Mach. Tools Manuf., 36/12, 1996. p. 1401−1411.

[10] Horejš O., Mareš M., Hornych J. Real-time compensation of machine tool thermal error including cutting process. Journal of Machine Engineering, 15/3, 2015. p. 5-18.

[11] Ljung L. System identification toolbox 7 User's guide, 2009.